

MIT Open Access Articles

Nonparametric obstruction detection for UWB localization

The MIT Faculty has made this article openly available. **Please share** how this access benefits you. Your story matters.

Citation: Marano, S. et al. "Nonparametric Obstruction Detection for UWB Localization." Global Telecommunications Conference, 2009. GLOBECOM 2009. IEEE. 2009. 1-6. ©2009 IEEE.

As Published: <http://dx.doi.org/10.1109/GLOCOM.2009.5425460>

Publisher: Institute of Electrical and Electronics Engineers

Persistent URL: <http://hdl.handle.net/1721.1/59985>

Version: Final published version: final published article, as it appeared in a journal, conference proceedings, or other formally published context

Terms of Use: Article is made available in accordance with the publisher's policy and may be subject to US copyright law. Please refer to the publisher's site for terms of use.



Nonparametric Obstruction Detection for UWB Localization

Stefano Maranò*, Wesley M. Gifford[†], Henk Wymeersch[‡], and Moe Z. Win[†]

*Swiss Seismological Service, ETH Zürich, Zürich, Switzerland

Email: stefano.marani@sed.ethz.ch

[†]Laboratory for Information and Decision Systems, Massachusetts Institute of Technology, Cambridge, MA 02139

Email: wgifford@mit.edu, moewin@mit.edu

[‡]Chalmers University of Technology, Göteborg, Sweden

Email: henk.wymeersch@ieee.org

Abstract—Ultra-wide bandwidth (UWB) transmission is a promising technology for indoor localization due to its fine delay resolution and obstacle-penetration capabilities. However, the presence of walls and other obstacles introduces a positive bias in distance estimates, severely degrading localization accuracy. We have performed an extensive indoor measurement campaign with FCC-compliant UWB radios to quantify the effect of non-line-of-sight (NLOS) propagation. Based on this campaign, we extract key features that allow us to distinguish between NLOS and LOS conditions. We then propose a nonparametric approach based on support vector machines for NLOS identification, and compare it with existing parametric (i.e., model-based) approaches. Finally, we evaluate the impact on localization through Monte Carlo simulation. Our results show that it is possible to improve positioning accuracy relying solely on the received UWB signal.

Index Terms—NLOS Identification, Support Vector Machine, UWB.

I. INTRODUCTION

Location-awareness is fast becoming a fundamental aspect of wireless networks and will enable a myriad of applications, in both the commercial and the military sectors [1]. Ultra-wide bandwidth (UWB) transmission provides robust signaling, as well as through-wall propagation and high-resolution ranging capabilities [2], [3]. Therefore, UWB is a promising technology for location-aware applications in harsh environments with stringent operational requirements [4], [5], such as indoor navigation and simultaneous localization and mapping (SLAM).

A number of implementation challenges remain before UWB systems can be deployed on a large scale. These include signal acquisition, multi-user interference, multipath effects, and non-line-of-sight (NLOS) propagation. The latter issue is especially critical for high-resolution location-aware applications, since NLOS propagation introduces positive biases in distance estimation algorithms, which can seriously affect the localization performance [3], [6]. Typical harsh environments such as enclosed areas, urban canyons, or tree canopies inherently have a high occurrence of NLOS situations. It is therefore critical to: (i) understand the impact of NLOS conditions on localization systems; and (ii) develop techniques that counter their effects.

A typical localization system comprises two stages: a ranging stage and a localization stage. In the ranging stage, signals are exchanged between devices, based on which relative angles or distances can be estimated. This relative position information is commonly based on signal arrival times (assuming a known propagation speed) or received signal power (assuming a known path loss). In the localization stage, the relative position information is combined with absolute position information (e.g., anchor positions) resulting in a position estimate. NLOS propagation impacts the ranging stage, since signals propagating through materials undergo an additional delay and power reduction. Moreover, when the direct line-of-sight (LOS) path is completely blocked, signals that arrive at the receiver via reflected paths, also exhibit delays and power reductions. In either case, any distance estimates in NLOS conditions will be positively biased.

NLOS identification attempts to distinguish between LOS¹ and NLOS conditions, and is commonly based on range estimates, on the channel impulse response (CIR), or on coarse position estimates [7]–[11]. The first class of techniques relies on the analysis of a history of range estimates, and often requires a large number of observations, which results in significant latency [7]–[9]. The second class of techniques relies on a single received signal, based on which the channel is identified as being either LOS or NLOS [10]. No additional latency is incurred. In [10], a likelihood ratio test is proposed to discriminate between the LOS and NLOS condition, based on statistics extracted from the channel response, and is evaluated using the IEEE 802.15.4a channel model. The third class of techniques combines range estimates from different sources to compute a coarse position estimate. When there is sufficient redundancy, NLOS estimates can be identified [11]. A detailed overview of NLOS identification techniques can be found in [8]. We note that all these works on NLOS identification are based on statistical techniques or on ad-hoc methods.

In this paper, we propose a *nonparametric approach* using machine learning techniques that does not require any

¹Throughout this paper the term LOS is used to denote the existence of a *visual* LOS. Specifically, a signal is considered as LOS when the straight line between the transmitting and receiving antenna is unobstructed.

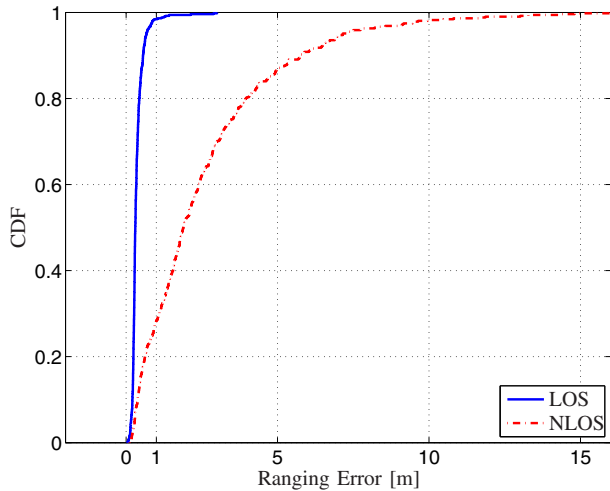


Fig. 1. CDF of the ranging error for the LOS and NLOS conditions.

statistical characterization of LOS and NLOS channels. Furthermore, our approach is based directly on the UWB CIR and thus avoids any latency issues. To validate our identification algorithms, we use results from a recent indoor measurement campaign with FCC-compliant UWB radios, rather than relying on statistical channel models. Hence, our results give a realistic indication of real-world performance. We evaluate the performance of our proposed techniques, both in terms of identification error rate and in terms of localization performance, and compare with existing techniques.

The remainder of this paper is organized as follows. In Section II we briefly describe the measurement campaign. In Section III we detail different approaches to NLOS detection, including our novel nonparametric method. In Section IV we provide detailed numerical results, followed by our conclusions in Section V.

II. MEASUREMENT CAMPAIGN

During Fall 2007 the Wireless Communication and Network Sciences Laboratory performed a detailed measurement campaign at the Massachusetts Institute of Technology. The measurements were made with two small radios capable of performing communications and ranging using impulse-radio UWB signals. Each radio complies with the emission limit set forth by the FCC [12] and has a 10 dB bandwidth from 3.1 GHz to 6.3 GHz. The radio runs a round-trip time-of-arrival ranging protocol and is capable of simultaneously capturing a waveform. Each waveform, which is affected by thermal noise, is sampled with $T_{\text{sample}} = 41.3$ ps over an observation window of $T = 190$ ns.

Measurements were taken at over 1000 transmitter/receiver locations in an indoor office environment [13]. Since the primary focus of this work is the impact of obstructions, measurement positions were chosen so that half of the collected waveforms were transmitted under NLOS conditions. The distance between transmitter and receiver varied from roughly 0.6 m up to 18 m, in an attempt to capture a wide variety

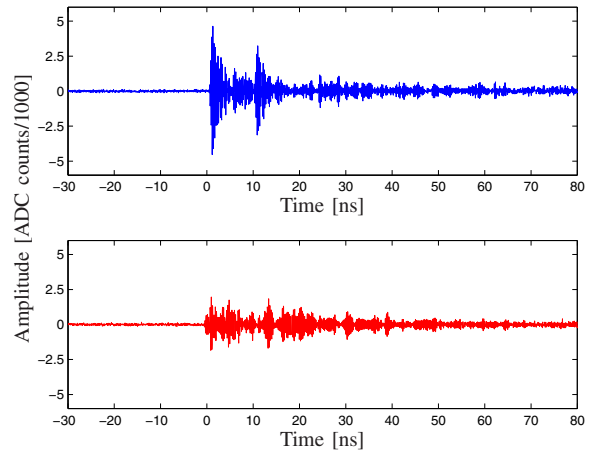


Fig. 2. In some situations there is a clear difference between LOS (upper waveform) and NLOS (lower waveform) signals.

of operating conditions. Along with the received waveform, the associated range estimate and the actual distance were recorded. The final database includes 1024 measurements, 512 LOS and 512 NLOS.

III. OBSTRUCTION DETECTION

The collected measurement data illustrates that NLOS propagation conditions significantly impact ranging performance. Fig. 1 shows the empirical cumulative distribution functions (CDFs) of the ranging error under the two different channel conditions. In LOS conditions the ranging error is below one meter in more than 95% of the measurements. On the other hand, in NLOS conditions the ranging error is below one meter in less than 30% of the measurements.

In this section, we develop techniques to distinguish between LOS and NLOS conditions. Our techniques are nonparametric, and use a low-complexity least squares support vector machine (LS-SVM) [14], [15]. We first describe the features we use to distinguish between LOS and NLOS situations, followed by a conventional parametric solution to NLOS identification [10]. We then give a brief introduction of LS-SVM, and describe how it can be used for NLOS identification in localization applications.

A. Features

We have extracted a number of features from every received waveform $r(t)$, which we expect to capture the salient differences between LOS and NLOS signals. These features were selected based on the following observations: (i) due to reflections or obstructions, NLOS signals are considerably more attenuated and present smaller energy and amplitude; (ii) in LOS signals the strongest path typically corresponds to the first path, while in the NLOS case some weak components precede the strongest path, resulting in a longer rise time; and (iii) the root-mean-square (RMS) delay spread, which captures the temporal dispersion of the energy in a signal, is larger in NLOS signals. Fig. 2 depicts two waveforms received in

the LOS and NLOS conditions supporting our observations. We also include some features that have been presented in the literature. Taking these considerations into account, the features we will consider are as follows:²

- 1) *Energy of the received signal*: $\mathcal{E}_r = \int_{-\infty}^{+\infty} |r(t)|^2 dt$.
- 2) *Maximum amplitude of the received signal*: $r_{\max} = \max_t |r(t)|$.
- 3) *Rise time*:

$$t_{\text{rise}} = t_{\text{H}} - t_{\text{L}},$$

where $t_{\text{L}} = \min_t \{t : |r(t)| \geq \alpha \sigma_n\}$, $t_{\text{H}} = \min_t \{t : |r(t)| \geq \beta r_{\max}\}$, and σ_n is the standard deviation of the thermal noise. The values of $\alpha > 0$ and $0 < \beta \leq 1$ are chosen empirically; in our case, we used $\alpha = 6$ and $\beta = 0.6$.

- 4) *Mean excess delay*: $\tau_{\text{MED}} = \int_{-\infty}^{+\infty} t\psi(t) dt$, where $\psi(t) = |r(t)|^2 / \mathcal{E}_r$.
- 5) *RMS delay spread (RMS-DS)*:

$$\tau_{\text{RMS}} = \int_{-\infty}^{+\infty} (t - \tau_{\text{MED}})^2 \psi(t) dt.$$

- 6) *Kurtosis*:

$$\kappa = \frac{1}{\sigma_{|r|}^4 T} \int_T (|r(t)| - \mu_{|r|})^4 dt,$$

where $\mu_{|r|} = \frac{1}{T} \int_T |r(t)| dt$ and $\sigma_{|r|}^2 = \frac{1}{T} \int_T (|r(t)| - \mu_{|r|})^2 dt$.

B. Parametric NLOS Identification

In [10], a likelihood ratio test was proposed to discriminate between the LOS and NLOS conditions. A database of channel responses was generated from the IEEE 802.15.4a channel model. Three statistical measures were extracted from each channel response $r(t)$: the kurtosis κ , the RMS-DS τ_{RMS} , and the MED τ_{MED} . The probability density function (PDF) of these features for both LOS and NLOS conditions were modeled by log-normal distributions, with parameters depending on the specific IEEE channel model. For any specific feature we can distinguish between LOS and NLOS through a likelihood-ratio test (LRT). In order to use all the features jointly, the joint PDF of the three features is required. Since this joint PDF is hard to obtain, a suboptimal solution, which was proposed in [10], is to consider the three features as independent, leading to the following LRT:

$$\frac{f_{\kappa}(\kappa|\text{LOS})}{f_{\kappa}(\kappa|\text{NLOS})} \times \frac{f_{\tau_{\text{MED}}}(\tau_{\text{MED}}|\text{LOS})}{f_{\tau_{\text{MED}}}(\tau_{\text{MED}}|\text{NLOS})} \times \frac{f_{\tau_{\text{RMS}}}(\tau_{\text{RMS}}|\text{LOS})}{f_{\tau_{\text{RMS}}}(\tau_{\text{RMS}}|\text{NLOS})} \stackrel{\text{LOS}}{\geq} 1. \quad (1)$$

We emphasize that the parametric approach relies on modeling the conditional distributions of the features under LOS

²The waveforms were processed to align the first path in the delay domain using a simple threshold-based detector.

and NLOS propagation conditions, invoking an independence assumption among features. When features are highly correlated, the independence assumption no longer holds, resulting in degraded performance. Furthermore, the parameters for the log-normal distributions are different for different IEEE channel models, thus requiring a higher-level classification during operation. To avoid these issues, we now develop a nonparametric identification technique that does not rely on any assumptions regarding the underlying distributions of the features, nor their independence. Hence, it is easily extended to various propagation scenarios and many types of features.

C. Nonparametric NLOS Identification

Support vector machines (SVMs) are supervised learning techniques used in classification problems [16], [17]. Arguably, SVM represents one of the most used classification techniques because of its robustness, its rigorous underpinning, its sparse solution, the fact that it requires few user-defined parameters, and its superior performance compared to other techniques such as neural networks. In this work the least squares SVM (LS-SVM) technique is employed. LS-SVM is a low-complexity variation of the standard SVM, and has been applied successfully to classification and regression problems [14], [15].

In this paper, we define a classifier as a function $\mathbb{R}^n \rightarrow \{-1, +1\}$ of the form

$$l(\mathbf{x}) = \text{sign}[y(\mathbf{x})] \quad (2)$$

with

$$y(\mathbf{x}) = \mathbf{w}^T \varphi(\mathbf{x}) + b \quad (3)$$

where $\varphi(\cdot)$ is a predetermined function, \mathbf{x} is the classifier input, and \mathbf{w} and b are unknown parameters of the classifier. These parameters are estimated based on a training set $\{\mathbf{x}_k, l_k\}_{k=1}^N$, with inputs $\mathbf{x}_k \in \mathbb{R}^n$ and labels $l_k \in \{-1, +1\}$. In our case, $l_k = -1$ corresponds to a NLOS waveform, $l_k = +1$ corresponds to a LOS waveform, and \mathbf{x} is a set of features extracted from the waveform. The LS-SVM classifier is a maximum-margin³ classifier, obtained by solving the following constrained optimization problem:

$$\begin{aligned} \arg \min_{\mathbf{w}, b, \mathbf{e}} \quad & \frac{1}{2} \|\mathbf{w}\|^2 + \gamma \frac{1}{2} \|\mathbf{e}\|^2 \\ \text{s.t.} \quad & l_k y(\mathbf{x}_k) = 1 - e_k, \forall k \end{aligned} \quad (4)$$

where γ controls the trade-off between minimizing the errors and model complexity. The dual turns out to be a linear program (LP):

$$\begin{bmatrix} 0 & \mathbf{1}^T \\ \mathbf{1} & \mathbf{\Omega} + \mathbf{I}/\gamma \end{bmatrix} \begin{bmatrix} b \\ \boldsymbol{\alpha} \end{bmatrix} = \begin{bmatrix} 0 \\ \mathbf{1}_N \end{bmatrix} \quad (6)$$

where $\boldsymbol{\alpha}$ is a vector of Lagrange multipliers, $\mathbf{\Omega}$ is an $N \times N$ matrix with $\Omega_{kl} = y_k y_l K(\mathbf{x}_k, \mathbf{x}_l)$, and $K(\mathbf{x}_k, \mathbf{x}_l) =$

³The *margin* is given by $1/\|\mathbf{w}\|$, and is defined as the smallest distance between the decision boundary $\mathbf{w}^T \varphi(\mathbf{x}) + b = 0$ and any of the training samples $\varphi(\mathbf{x}_k)$.

$\varphi(\mathbf{x}_k)^T \varphi(\mathbf{x}_l)$ is the kernel function. Solving the LP in (6) yields the LS-SVM classifier, which is of the form:

$$l(\mathbf{x}) = \text{sign} \left\{ \sum_{k=1}^N \alpha_k l_k K(\mathbf{x}, \mathbf{x}_k) + b \right\}. \quad (7)$$

D. Localization with NLOS identification

Once the agent has estimated distances with respect to $N_b \geq 3$ anchor nodes, it can estimate its location, using the anchor positions and estimated distances.⁴ While there are many algorithms that can achieve this goal, we focus on the least squares (LS) technique, due to its simplicity and because it makes no assumptions regarding the ranging error model. The agent can infer its position by minimizing the LS cost function:

$$\hat{\mathbf{p}} = \arg \min_{\mathbf{p}} \left\{ \sum_{i=1}^{N_b} w_i \left(\hat{d}_i - \|\mathbf{p} - \mathbf{p}_i\| \right)^2 \right\} \quad (8)$$

where \mathbf{p}_i is the position of i -th anchor and w_i is a weight parameter, to be detailed below. In (8), some of the estimates \hat{d}_i may correspond to NLOS conditions, adversely affecting the final LS position estimate. Here, we investigate three localization strategies that set the weights w_i based on the outcome of the classifier.

- 1) *Standard*: All the N_b range estimates \hat{d}_i from neighboring anchor nodes are used by the LS algorithm for localization. Weights are set $w_i = 1$ for $1 \leq i \leq N_b$.
- 2) *Identification*: Signals associated with range estimates are classified as LOS or NLOS using a classifier such as (1) or (7), based on a set of features \mathbf{x} . Range estimates are used by the localization algorithm only if the associated signal was classified as LOS, while NLOS signals are discarded. This gives the following weights:

$$w_i = \begin{cases} 1 & l(\mathbf{x}) = +1 \\ 0 & l(\mathbf{x}) = -1 \end{cases} \quad (9)$$

Note that three anchor nodes is the minimum number of nodes needed to localize in a two-dimensional scenario. Therefore, whenever less than three w_i are set to one, the agent is unable to localize. In this case, we set the localization error to $+\infty$.

- 3) *Ranking*: Estimated distances are ranked according to the soft-output of the LS-SVM classifier $\sum_{k=1}^N \alpha_k l_k K(\mathbf{x}, \mathbf{x}_k) + b$. The three estimates with highest ranking are retained. The weights are set $w_i = 1$ for the three largest soft outputs, and the remaining weights are set to zero.

IV. NUMERICAL RESULTS AND DISCUSSION

In this section, we present our numerical results. In section IV-A, performance for the parametric and the proposed nonparametric approach are reported in terms of classification error rates. In section IV-B, localization performance is given for simulated networks consisting of one agent and five anchors.

⁴Provided that the anchors are not collinear.

A. Identification Performance

The performance of a LOS/NLOS identification algorithm can be assessed through the false alarm probability and the missed detection probability. The false alarm probability, or the probability that NLOS is chosen when the true condition is LOS, is given by $P_{\text{FA}} = \mathbb{P}\{l(\mathbf{x}) = -1 | l_k = +1\}$. The missed detection probability, or the probability that LOS is chosen when the true condition is NLOS, is given by $P_{\text{M}} = \mathbb{P}\{l(\mathbf{x}) = +1 | l_k = -1\}$. We use 10-fold cross-validation, where part of our database is used for training, and the remaining part of the database is used for validation.

1) *Parametric classification*: As a benchmark, we evaluate the approach from [10] (see also section III-B), using the kurtosis κ , the RMS-DS τ_{RMS} , and the MED τ_{MED} in a LRT (1).⁵ The resulting error rates are $P_{\text{FA}} = 0.18$ and $P_{\text{M}} = 0.14$, leading to an overall correct classification rate of 84%.

2) *Nonparametric classification*: In a nonparametric approach using the LS-SVM, we can use any subset of features from section III-A without needing an explicit statistical model. Through an exhaustive search, we can easily find the set of features which has the smallest error probability. Fig. 3 shows the performance of classifiers based on every possible feature set of size three.⁶ The set corresponding to column 7 in Fig. 3 (consisting of energy \mathcal{E}_r , rise time t_{rise} , and kurtosis κ) yields the best performance: $P_{\text{FA}} = 0.08$ and $P_{\text{M}} = 0.09$, leading to an overall correct classification rate of 91%. The set of features from [10] corresponds to column 20, and turns out to be the worst set of size three, in terms of overall performance. For larger sets, performance does not noticeably improve, while for smaller sets performance is degraded (results not shown). Hence, the set \mathcal{E}_r , t_{rise} , and κ provides a good complexity/performance trade off.

3) *Discussion*: Less than 10% of the waveforms were wrongly classified by the LS-SVM classifier. It turns out that LOS waveforms that are classified as NLOS occur under a few specific propagation conditions: (i) obstruction of a large portion of the Fresnel zone; (ii) presence of strong reflected paths, with amplitude comparable to the first path; and (iii) transmission over a large distance. Conversely, some NLOS waveforms are classified as LOS when the obstructions consist of relatively thin plaster or glass walls, or when propagation is over very short distances. The previous qualitative considerations allow us to obtain insight into the classification errors encountered and provide a meaningful explanation for those errors.

Fig. 4 shows a graphical representation of all the feature values, as well as the classification errors. The upper half of the figure (waveforms 1-512) corresponds to the LOS waveforms, while the lower part corresponds to the 512 NLOS waveforms. The first six columns show the normalized feature values, and the seventh column shows the results of the classification (blue for correct classification, red for incorrect classification, based

⁵In a Bayesian setting, the threshold equal to 1 corresponds to equal a priori occurrence of LOS and NLOS.

⁶For reasons of numerical stability, features are converted to the log-domain before training and evaluating the LS-SVM.

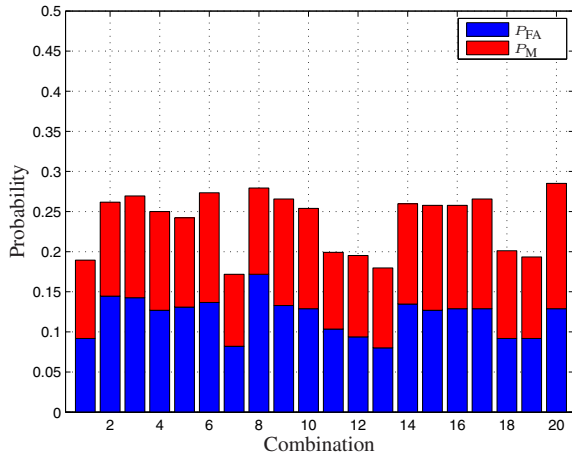


Fig. 3. The error probabilities P_{FA} and P_M for NLOS identification using LS-SVM with every combination of three features. It should be noted that $P_{FA} + P_M$ equals two times the error probability.

on the LS-SVM with features \mathcal{E}_r , t_{rise} , and κ). We observe that classification errors often correspond to atypical feature values. Also, we see that errors appear in clusters. This is because adjacent waveforms were captured under similar propagation conditions and in nearby locations.

B. Localization Performance

We evaluate the localization performance for a system with one agent (at unknown position $\mathbf{p} = (0, 0)$), $N_b = 5$ anchors, and a varying probability of NLOS condition $0 \leq P_{NLOS} \leq 1$ for 5000 network realizations. For every anchor i ($1 \leq i \leq N_b$), we draw a waveform from the database as follows: with probability P_{NLOS} we draw from the NLOS database and with probability $1 - P_{NLOS}$ from the LOS database. The true distance d_i corresponding to that waveform is then used to place the i -th anchor at position $\mathbf{p}_i = (d_i \sin(2\pi(i-1)/N_b), d_i \cos(2\pi(i-1)/N_b))$, while the estimated distance \hat{d}_i is provided to the agent. The agent estimates its position using a gradient descent technique to minimize the LS cost function from Section III-D, with an initial position estimate $\hat{\mathbf{p}}^{(0)}$ given by the arithmetic mean of the anchor positions.

To capture the accuracy and availability of localization, we employ the notion of *outage probability* [18]. For a certain P_{NLOS} and a certain allowable error e_{th} (say, 2 m), the agent is said to be in outage when its position error $\|\mathbf{p} - \hat{\mathbf{p}}\|$ exceeds e_{th} :

$$P_{out}(e_{th}) = \mathbb{E} \{ \mathbb{I} \{ \|\mathbf{p} - \hat{\mathbf{p}}\| > e_{th} \} \} \quad (10)$$

where $\mathbb{I} \{ \mathcal{P} \}$ is the indicator function, which, for a proposition \mathcal{P} , is zero when \mathcal{P} is false and one otherwise. The expectation in (10) can then be approximated through Monte Carlo simulations, by counting the number of times an outage occurs.

Figure 5 depicts the outage probability as a function of the allowable error e_{th} , for $P_{NLOS} = 0.2$. We see that even with just 20% of the anchors in NLOS condition (on average), the *standard* technique performs quite poorly. The *identification*

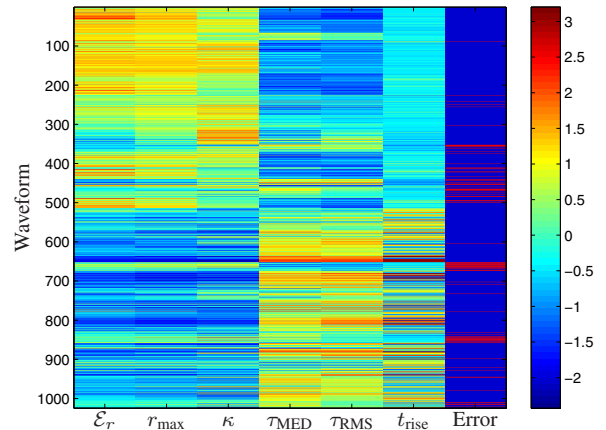


Fig. 4. Graphical depiction of the feature values after normalization (zero mean and unit variance) and classification result (red indicates incorrect classification).

technique using parametric classification can improve the performance. Using the nonparametric classification, additional performance gains are achievable, since we can more reliably discard NLOS distance estimates. Observe that for both identification techniques, the outage probability saturates as e_{th} increases, leading to an outage floor. This behavior occurs because there is a non-zero probability that less than three anchors are identified as LOS, in which case the agent declares itself in outage for any e_{th} . On the other hand, the *standard* technique always uses information from *all* 5 anchors, so that outage curves do not saturate for the considered range of e_{th} . This implies that the *standard* technique will outperform the *identification* techniques as e_{th} increases, as can be seen in Fig. 5. Finally, the *ranking* technique combines the ability to identify NLOS waveforms with the usage of three anchors, and has the best overall performance.

In Fig. 6 the allowable error is fixed to $e_{th} = 2$ m, while the channel conditions vary from ideal, $P_{NLOS} = 0$, to extremely harsh, $P_{NLOS} = 1$. It can be seen that the *ranking* technique has the best performance in all possible channel conditions, while the *identification* techniques outperform the *standard* technique only for P_{NLOS} below approximately 0.5. This illustrates that while improving classification performance is important, there is information present in NLOS signals that should be exploited to improve localization performance. Classification can serve as an initial step, the results of which can be used in a localization algorithm. With knowledge of NLOS conditions, the localization algorithm can then take the steps necessary to most effectively use the available information and achieve the best performance.

V. CONCLUSION

The ability to distinguish between LOS and NLOS propagation is important for location-aware applications such as indoor navigation and SLAM. In this paper, we have presented a novel nonparametric technique to identify NLOS propagation

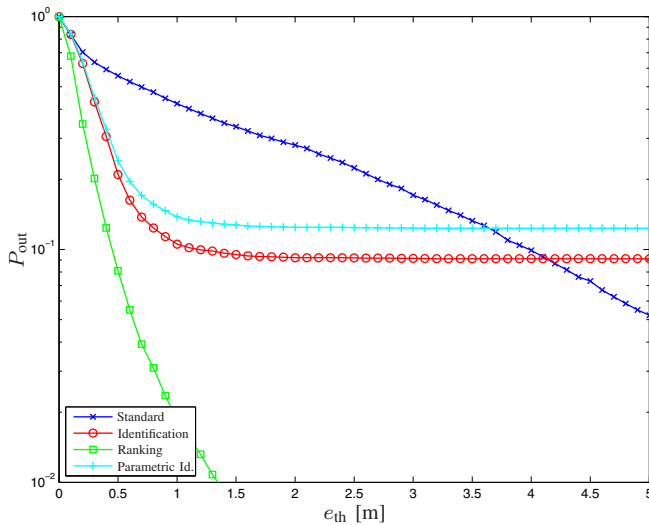


Fig. 5. Outage probability for $N_b = 5$, with $P_{NLOS} = 0.2$.

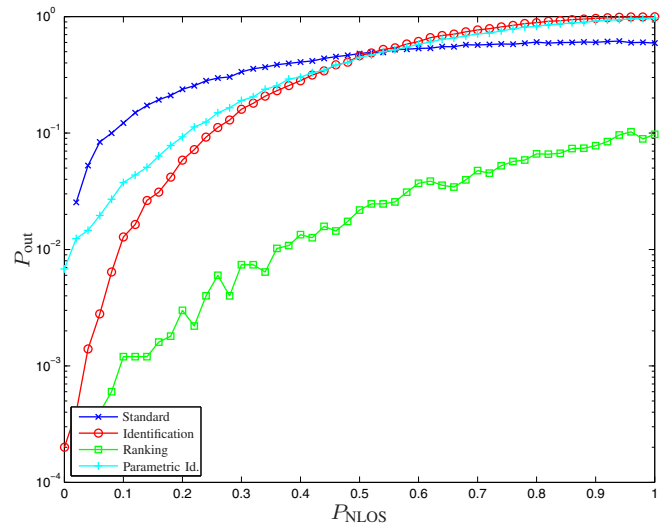


Fig. 6. Outage probability for $N_b = 5$, with $e_{th} = 2$ m.

conditions in UWB communication systems. The proposed technique relies solely on received UWB waveforms, through a set of features that capture the salient differences between LOS and NLOS conditions. Contrary to existing parametric approaches, our technique does not rely on any statistical models, and has superior classification performance. Our results were validated by an extensive indoor measurement campaign made with FCC-compliant UWB radios. As a next step, we will develop classification techniques that are able to provide Bayesian information to the localization algorithms, so that we can optimally fuse all the available information.

VI. ACKNOWLEDGMENTS

The authors wish to thank the following people for their help during the measurement campaign: U. Ferner, O. Hernandez, P. Pinto, T. Quek, Y. Shen, W. Suwansantisuk, H. Tang, and K. Woradit.

This research was supported, in part, by the National Science Foundation under Grants ECCS-0636519 and ECCS-0901034, the Office of Naval Research Presidential Early Career Award for Scientists and Engineers (PECASE) N00014-09-1-0435, the Defense University Research Instrumentation Program under Grant N00014-08-1-0826, and the MIT Institute for Soldier Nanotechnologies.

REFERENCES

- [1] N. Patwari, J. N. Ash, S. Kyperountas, A. O. Hero, III, R. L. Moses, and N. S. Correal, "Locating the nodes: cooperative localization in wireless sensor networks," *IEEE Signal Process. Mag.*, vol. 22, no. 4, pp. 54–69, Jul. 2005.
- [2] D. Dardari, A. Conti, U. J. Ferner, A. Giorgetti, and M. Z. Win, "Ranging with ultrawide bandwidth signals in multipath environments," *Proc. IEEE*, vol. 97, no. 2, pp. 404–426, Feb. 2009, special issue on *Ultra-Wide Bandwidth (UWB) Technology & Emerging Applications*.
- [3] S. Gezici, Z. Tian, G. B. Giannakis, H. Kobayashi, A. F. Molisch, H. V. Poor, and Z. Sahinoglu, "Localization via ultra-wideband radios: a look at positioning aspects for future sensor networks," *IEEE Signal Process. Mag.*, vol. 22, pp. 70–84, Jul. 2005.
- [4] M. Z. Win and R. A. Scholtz, "Impulse radio: How it works," *IEEE Commun. Lett.*, vol. 2, no. 2, pp. 36–38, Feb. 1998.

- [5] —, "Ultra-wide bandwidth time-hopping spread-spectrum impulse radio for wireless multiple-access communications," *IEEE Trans. Commun.*, vol. 48, no. 4, pp. 679–691, Apr. 2000.
- [6] J.-Y. Lee and R. A. Scholtz, "Ranging in a dense multipath environment using an UWB radio link," *IEEE J. Sel. Areas Commun.*, vol. 20, no. 9, pp. 1677–1683, Dec. 2002.
- [7] J. Borras, P. Hatrack, and N. B. Mandayam, "Decision theoretic framework for NLOS identification," in *Proc. 48th Annual Int. Veh. Technol. Conf.*, vol. 2, Ottawa, Canada, May 1998, pp. 1583–1587.
- [8] J. Schroeder, S. Galler, K. Kyamakya, and K. Jobmann, "NLOS detection algorithms for ultra-wideband localization," *Positioning, Navigation and Communication, 2007. WPNC '07. 4th Workshop on*, pp. 159–166, Mar. 2007.
- [9] S. Gezici, H. Kobayashi, and H. V. Poor, "Non-parametric non-line-of-sight identification," in *Proc. IEEE Semiannual Veh. Technol. Conf.*, vol. 4, Orlando, FL, Oct. 2003, pp. 2544–2548.
- [10] I. Guvenc, C.-C. Chong, and F. Watanabe, "NLOS identification and mitigation for UWB localization systems," in *Proc. IEEE Wireless Commun. and Networking Conf.*, Kowloon, China, Mar. 2007, pp. 1571–1576.
- [11] M. Tüchler and A. Huber, "An improved algorithm for UWB-based positioning in a multi-path environment," *Communications, 2006 International Zürich Seminar on*, pp. 206–209, 2006.
- [12] Federal Communications Commission, "Revision of part 15 of the commission's rules regarding ultra-wideband transmission systems, first report and order (ET Docket 98-153)," Adopted Feb. 14, 2002, Released Apr. 22, 2002.
- [13] A. F. Molisch, "IEEE 802.15.4a channel model - final report," 2005. [Online]. Available: <ftp://ftp.802wirelessworld.com/15/05>
- [14] J. A. K. Suykens and J. Vandewalle, "Least squares support vector machine classifiers," *Neural Processing Letters*, vol. 9, no. 3, pp. 293–300, Jun. 1999.
- [15] J. A. K. Suykens, T. Van Gestel, J. De Brabanter, B. De Moor, and J. Vandewalle, *Least Squares Support Vector Machines*. World Scientific, 2002.
- [16] C. Cortes and V. Vapnik, "Support-vector networks," *Machine Learning*, vol. 20, no. 3, pp. 273–297, 1995.
- [17] C. J. Burges, "A tutorial on support vector machines for pattern recognition," *Data Mining and Knowledge Discovery*, vol. 2, pp. 121–167, 1998.
- [18] H. Wymeersch, J. Lien, and M. Z. Win, "Cooperative localization in wireless networks," *Proc. IEEE*, vol. 97, no. 2, pp. 427–450, Feb. 2009, special issue on *Ultra-Wide Bandwidth (UWB) Technology & Emerging Applications*.